# Maximum power and the corresponding efficiency for a Carnot-like thermoelectric cycle based on fluctuation theorem

Yuchao Hua, Zeng-Yuan Guo

# Maximum Power and The Corresponding Efficiency for A Carnot-like Thermoelectric Cycle Based on Fluctuation Theorem

Yuchao Hua[a]*, Zeng-Yuan Guo[b]

[a] Nantes Université, Laboratoire de thermique et énergie de Nantes, LTeN, F-44000 Nantes, France;

[b] Tsinghua Uuniversity, Department of Engineering Mechanics, 100084, Beijing, China;

*Corresponding author: Email: yuchao.hua@univ-nantes.fr

Here, we investigate the maximum power and efficiency of thermoelectric generators through devising a set of protocols for the isothermal and adiabatic processes of thermoelectricity to build a Carnot-like thermoelectric cycle, with the analysis based on fluctuation theorem (FT). The Carnot efficiency can be readily obtained for the quasi-static thermoelectric cycle with vanishing power. The maximum power-efficiency pair of the finite-time thermoelectric cycle is derived, which is found to have the identical form to that of Brownian motors characterized by the stochastic thermodynamics. However, it is of significant discrepancy compared to the linear-irreversible and endoreversible-thermodynamics-based formulations. The distinction with the linear-irreversible-thermodynamics case could result from the difference in the definitions of Peltier and Seebeck coefficients in the thermoelectric cycle. As for the endoreversible thermodynamics, we argue the applicability of endoreversibility could be questionable for analyzing the Carnot-like thermoelectric cycle, due to the incompatibility of the endoreversible hypothesis that attributes the irreversibility to finite heat transfer with thermal reservoirs, though the distinction in the mathematical expressions can vanish with the assumption that the ratio of thermoelectric power factors at the high and low temperatures ($\gamma$) is equal to the square root of the temperature ratio, $\gamma = \sqrt{T_{\mathrm{L}}/T_{\mathrm{H}}}$ (this condition could significantly deviate from the practical case). Lastly, utilizing our models as a concise tool to evaluate the maximum power-efficiency pairs of realistic thermoelectric material is presented with a case study on the n-type Silicon.

**Key words**: Thermoelectric, Maximum power, Efficiency, Irreversible,

Thermodynamics, Fluctuation theorem

# I. Introduction

Thermoelectricity has long been a highly active research topic, which holds a great potential to create solid-state energy converters capable of converting heat into electricity without moving components [1][2][3]. Furthermore, thermoelectric generator (TEG) can also serve as very crucial paradigmatic model for the researches of irreversible thermodynamics, like Onsager reciprocal relations (ORRs) [4], and the efficiency at maximum power [5], etc.

Currently, the linear-irreversible thermodynamics has been the major tool for analyzing TEGs and set the fundamental principles of thermoelectric research [2][6], which adopts the linear phenomenological relations within the framework of ORRs. As for the maximum power and the corresponding efficiency of thermoelectricity, Tab. 1 gives the widely-recognized formulations based on the linear-irreversible thermodynamics: the maximum power, $P_{\mathrm{Max\_LIRR}}$, is proportional to the power factor (PF, denoted by the symbol $P_{\mathrm{F}}$), the square of temperature difference $(T_{\mathrm{H}}-T_{\mathrm{L}})^2$, and a factor 1/4, while the efficiency (denoted by $\eta_{\mathrm{LIRR}}$) at max power is the half of Carnot efficiency ($\eta_{\mathrm{C}}$).

The other theoretical tool should be endoreversible thermodynamics [7][8]. Its core assumption, that is, the endoreversibility, reads: the irreversibility emerges merely owing to the finite heat exchange with heat reservoirs, while working substance is internally reversible and thus able to convert heat to work under Carnot

efficiency. This methodology has been extensively employed to handle various finite-time heat-engine cycles (mainly the fluid-based-mechanical-work systems) [8], and has derived the Curzon-Ahlborn (CA) efficiency ($\eta_{\mathrm{CA}}$, presented in Tab. 1) that is widely deemed to be generic for varied types of heat engines including TEGs [9][10]. The half of Carnot efficiency, predicted by the linear-irreversible thermodynamics, is regarded as the lower-bound of the CA efficiency formulation through its Taylor expansion with respect to $\eta_{\mathrm{C}}$ [10]. Much work has been conducted for recovering the CA efficiency in the framework of irreversible thermodynamics (linear and nonlinear) [5][9][10][11][12]. As for thermoelectricity, Apertet recovered the CA efficiency for a TEG in the limit of pure "external dissipation" [5]; Kaur et al. [12] constructed a TEG under the endoreversible assumption, by introducing the finite heat transfer relations between the TEG and heat reservoirs, and found that the use of Newton's cooling law can yield the CA efficiency. Additionally, as presented in Tab 1, the maximum power expressions obtained by these two methodologies hold significant difference: the endoreversible one ($P_{\mathrm{Max\_CA}}$) is proportional to the square of the difference between the square root of temperature $\left(\sqrt{T_{\mathrm{H}}}-\sqrt{T_{\mathrm{L}}}\right)^2$ and an effective heat conductance $K_{\mathrm{T}}$ determined by the specifics of the system. The maximum power of the endoreversible TEG by Kaur et al. [12] is of the identical temperature dependence, and its effective heat conductance $K_{\mathrm{T}}$ is merely dependent on the heat transfer coefficient rather than any thermoelectric coefficients (i.e., Seebeck or Peltier).

Furthermore, another distinct formulation for the efficiency at maximum power is derived for varied Brownian motors on the basis of stochastic thermodynamics

[13][14], $\eta_{\mathrm{ST}}$, as listed in Tab.1. Esposito et al. [15] proved that for the finite-time Carnot cycles not involving stochasticity, the lower and upper bounds of $\eta_{\mathrm{ST}}$ expression could be recovered under two limiting conditions, and the CA efficiency was also obtained in the case of symmetric dissipation. Particularly for thermoelectricity, Esposito et al. investigated a quantum-dot Carnot engine that undergoes the TEG-equivalent process using the master equation for the stochastic dynamics, and reached the similar conclusions to their previous work [10]. Moreover, following the methodology of phenomenological relations in irreversible thermodynamics, Apertet et al. [5] derived $\eta_{\mathrm{ST}}$ corresponding to the case of pure "internal dissipation" of a TEG. As for the maximum power based on the stochastic thermodynamics ($P_{\mathrm{Max\_ST}}$, listed in Tab. 1), it holds the same temperature dependence as $P_{\mathrm{Max\_LIRR}}$, with distinct factors (1/8 in $P_{\mathrm{Max\_ST}}$ and 1/4 in $P_{\mathrm{Max\_LIRR}}$), while the exact relation between the thermoelectric PF and the term $(\Delta S)^2\beta M$ remains to be clarified. Regarding the obvious discrepancy between $P_{\mathrm{Max\_ST}}$ and $P_{\mathrm{Max\_CA}}$, further investigation is also needed.

In the present work, we build a Carnot-like thermoelectric cycle through devising a set of protocols for the isothermal and adiabatic processes of thermoelectricity, which can serve a benchmark theoretical model to study the thermoelectric conversion. Its maximum power and corresponding efficiency in the case of finite-time operation are analyzed based on the fluctuation theorem (FT) [16][17][18][19]. Entropy production plays a key role when investigating the finite-time thermodynamic cycles [13][20]. Under some mild assumptions essentially

involving the microscale time reversal symmetry, the FT has been proven to be a powerful and generic theoretical tool to study the properties of the entropy production for various systems that are driven arbitrarily far from equilibrium states [16][17][18][19][21]. By contrast, some relatively strong assumptions regarding the thermoelectric transport process mechanisms, which may limit the generality, are generally required when employing the other theoretical methods: the ORR-constrained linear phenomenological relations for linear-irreversible thermodynamics [4][6], the formulation of the finite heat exchange with heat reservoirs for endoreversible thermodynamics [12], and the dynamic equations (e.g. the master equation) for stochastic thermodynamics [10]. Furthermore, the discrepancy for the formulations of maximum power and efficiency obtained from the different methodologies is discussed for thermoelectricity. Lastly, as a case study, the proposed models are applied to the n-type Silicon for estimating its maximum power-efficiency pairs.

TABLE 1 Expressions of the maximum power and the corresponding efficiency.

| | **Max power** | **Efficiency at Max power** | **Refs.** |
|---|---|---|---|
| Linear irreversible | $P_{\mathrm{Max\_LIRR}} = \frac{1}{4} P_{\mathrm{F}} (T_{\mathrm{H}} - T_{\mathrm{L}})^2$ | $\eta_{\mathrm{LIRR}} = \frac{1}{2}\eta_{\mathrm{C}}$ | Goupil et al. [6] Benenti et al. [20] |
| Endoreversible | $P_{\mathrm{Max\_CA}} = K_{\mathrm{T}}\left(\sqrt{T_{\mathrm{H}}} - \sqrt{T_{\mathrm{L}}}\right)^2$ | $\eta_{\mathrm{CA}} = 1 - \sqrt{T_{\mathrm{L}}/T_{\mathrm{H}}}$ | Hoffmann [8] Kaur et al. [12] |
| Stochastic | $P_{\mathrm{Max\_ST}} = \frac{1}{8}(\Delta S)^2 \beta M (T_{\mathrm{H}} - T_{\mathrm{L}})^2$ | $\eta_{\mathrm{ST}} = \frac{\eta_{\mathrm{C}}}{2 - \beta\eta_{\mathrm{C}}}$ | Schmiedl et al. [13] Fu et al. [14] |
| $T_{\mathrm{H}}$: high temperature; $T_{\mathrm{L}}$: low temperature; $P_{\mathrm{F}} = \alpha_{\mathrm{S}}^2/R_{\mathrm{e}}$: power factor; $\alpha_{\mathrm{S}}$: Seebeck coefficient; $R_{\mathrm{e}}$: electric resistance; $\eta_{\mathrm{C}} = 1 - T_{\mathrm{L}}/T_{\mathrm{H}}$: Carnot efficiency; $K_{\mathrm{T}}$: an effective heat conductance | | | |

dependent on the system; $\Delta S$: entropy change; $\beta$: a ratio between the dissipative couplings of cold and hot reservoirs; $M$: a coefficient dependent on the system.

## II. Carnot-Like Thermoelectric Cycle

Figure 1 illustrates the Temperature (T) – Entropy (S) diagram of Carnot cycle. For a TEG where the targeted thermoelectric system Ψ is assumed to hold constant volume, the thermoelectric cycle should involve four processes:

A → B: Isothermal process at $T_{\mathrm{H}}$ (the high temperature): As shown in Fig. 2, such process can be realized through keeping the targeted system Ψ in contact with a heat reservoir of temperature $T_{\mathrm{H}}$ constantly, and sequentially connecting and disconnecting Ψ to a series of electrochemical potential reservoirs $\mu_{i=1,\cdots N}$ where $\mu_1 = \mu_A$ and $\mu_N = \mu_B$, during a time interval $\tau$ , in analogy to Ref. [17]. The heat $Q_{\mathrm{AB}}$ is absorbed due to the Peltier effect, and the work $W_{AB}$ is extracted, which is calculated as,

$$W_{\mathrm{AB}} = -\int_0^{\tau} \mu(t) dN(t) = Q_{\mathrm{AB}} - (U_{\mathrm{B}} - U_{\mathrm{A}}) \tag{1}$$

where $\mu(t)$ is the targeted system's electrochemical potential at the time *t*, and $N(t)$ is its charge number at the time *t*. When the time interval $\tau \to \infty$, this process can be regarded as quasistatic.

B → C: Adiabatic process from $T_{\mathrm{H}}$ to $T_{\mathrm{L}}$ (the low temperature): As presented in Fig. 3, the targeted system Ψ is sequentially connected and disconnected to a series of reservoirs $\{T, \mu\}_{i=1,\cdots N}$ with $\{T, \mu\}_1 = \{T_{\mathrm{B}}, \mu_{\mathrm{B}}\}$ and $\{T, \mu\}_N = \{T_{\mathrm{C}}, \mu_{\mathrm{C}}\}$, during a time interval $\tau_{\mathrm{adia}}$. There are actually two means to keep the process ideally adiabatic, i.e. no heat exchange between the targeted system Ψ and the reservoirs: this state

transition happens instantaneously, $\tau_{\mathrm{adia}} \to 0$, or the thermal resistance ($R_{\mathrm{T}}$) between $\Psi$ and reservoirs is infinitely large, $R_{\mathrm{T}} \to \infty$. In any one of these two cases, the extracted work is equal to the difference of internal energy between the states C and B,

$$W_{\mathrm{BC}} = -(U_{\mathrm{C}} - U_{\mathrm{B}}) \tag{2}$$

$\mathrm{C} \to \mathrm{D}$: Isothermal process at $T_{\mathrm{L}}$: This process is operated following the identical protocol to $\mathrm{A} \to \mathrm{B}$, with changing the heat reservoir temperature to $T_{\mathrm{L}}$ and setting the electrochemical potential reservoirs as $\mu_1 = \mu_{\mathrm{C}}$ and $\mu_N = \mu_{\mathrm{D}}$. Here, we assume the duration of $\mathrm{C} \to \mathrm{D}$ is the same as that of $\mathrm{A} \to \mathrm{B}$. The heat $Q_{\mathrm{CD}}$ is released due to the Peltier effect, and the work $W_{\mathrm{CD}}$ can also be calculated following Eq. (1),

$$W_{\mathrm{AB}} = Q_{\mathrm{CD}} - (U_{\mathrm{D}} - U_{\mathrm{C}}) \tag{3}$$

$\mathrm{D} \to \mathrm{A}$: Adiabatic process from $T_{\mathrm{L}}$ to $T_{\mathrm{H}}$: It follows the operation of $\mathrm{B} \to \mathrm{C}$ with replacing the reservoirs as $\{T, \mu\}_1 = \{T_{\mathrm{D}}, \mu_{\mathrm{D}}\}$ and $\{T, \mu\}_N = \{T_{\mathrm{A}}, \mu_{\mathrm{A}}\}$, during the time interval $\tau_{\mathrm{adia}}$. Similarly, the work is given by $W_{\mathrm{DA}} = -(U_{\mathrm{A}} - U_{\mathrm{D}})$.

Therefore, employing the protocols depicted in Figs. 2 and 3, the thermoelectric cycle can be constructed as above, of which total work is given by,

$$\begin{aligned} W &= W_{\mathrm{AB}} + W_{\mathrm{BC}} + W_{\mathrm{CD}} + W_{\mathrm{DA}} \\ &= Q_{\mathrm{AB}} + Q_{\mathrm{CD}} \end{aligned} \tag{4}$$

As these two isothermal processes are quasistatic with $\tau \to \infty$, Eq. (4) becomes,

$$W = T_{\mathrm{H}}(S_{\mathrm{H}} - S_{\mathrm{L}}) + T_{\mathrm{L}}(S_{\mathrm{L}} - S_{\mathrm{H}}) = (T_{\mathrm{H}} - T_{\mathrm{L}})\Delta S. \tag{5}$$

with the Carnot efficiency,

$$\eta_{\mathrm{C}} = \frac{W}{Q_{\mathrm{AB}}} = 1 - \frac{T_{\mathrm{L}}}{T_{\mathrm{H}}}. \tag{6}$$

which is not surprising for a reversible thermoelectric cycle, due to the equivalence among heat engines [22].

## III. Finite-Time Carnot-Like Thermoelectric Cycle

When the thermoelectric cycle in Sec II operates within a finite time period, its efficiency will deviate from the Carnot formulation, due to entropy production [10], though those four state points are prescribed. A generally-adopted theorem is to add a term of irreversible work into the energy conservation equation to take the irreversibility into account [10][13],

$$W + W_{\mathrm{irr}} = (T_{\mathrm{H}} - T_{\mathrm{L}})\Delta S, \tag{7}$$

where the irreversible work $W_{\mathrm{irr}}$ is proportional to the entropy production supposed to be positive in general [13]. Nevertheless, it is noted that there is possibility of negative entropy production in some particular cases, like in small-scale systems [16][18]. Thus, instead of utilizing Eq. (7) directly, we start with clarifying the irreversibility in the cycle based on the methodology of fluctuation theorem (FT) [16][17][18][19].

In the thermoelectric cycle above, how the adiabatic processes are conducted and their irreversibility will not affect the work output, once they are ideally adiabatic. Therefore, the key issue should be the analysis of isothermal processes $\mathrm{A} \to \mathrm{B}$ and $\mathrm{C} \to \mathrm{D}$. As for an isothermal process of thermoelectric system that is realized

following the operation (or protocol) illustrated in Fig. 2, we could have a formulation that shares the generic form of Evans-Searles fluctuation theorem [18],

$$\frac{p\left(+\frac{\Delta\tilde{S}_{\mathrm{irr}}}{k_B}\right)}{p\left(-\frac{\Delta\tilde{S}_{\mathrm{irr}}}{k_B}\right)} = e^{\left(+\frac{\Delta\tilde{S}_{\mathrm{irr}}}{k_B}\right)} \tag{8}$$

where $k_B$ is Boltzmann constant, $\Delta\tilde{S}_{\mathrm{irr}}$ is the entropy production during the time interval, $p(\ \ )$ is the probability function for entropy production, and the label "∼" notes the entropy production is a process quantity that depends on how the process is operated. In fact, the protocol in Fig. 2 is devised in analogy to that presented in the paper by Jarzynski [17], which discussed the problem in canonical ensemble, while the present problem is about grand canonical ensemble. Due to the similar architectures of the protocols, it could not be nontrivial to derive Eq. (8) through replacing the canonical ensemble distribution to the grand canonical ensemble one following the identical methodology [23][24]. Therefore, the preconditions for the validity of Eq. (8) read [17],

- Evolution of the full phase space is Hamiltonian;
- Time reversal symmetry at microscale (no magnetic field);
- Weak coupling between the targeted system and the reservoirs.

In terms of Eq. (8), we have

$$\langle e^{\left(-\frac{\Delta\tilde{S}_{\mathrm{irr}}}{k_B}\right)}\rangle = \int p\left(+\frac{\Delta\tilde{S}_{\mathrm{irr}}}{k_B}\right) e^{\left(-\frac{\Delta\tilde{S}_{\mathrm{irr}}}{k_B}\right)} d\frac{\Delta\tilde{S}_{\mathrm{irr}}}{k_B} = \int p\left(-\frac{\Delta\tilde{S}_{\mathrm{irr}}}{k_B}\right) d\frac{\Delta\tilde{S}_{\mathrm{irr}}}{k_B} = 1. \tag{9}$$

Using Jensen's inequality, it is easily obtained,

$$\langle\Delta\tilde{S}_{\mathrm{irr}}\rangle \geq 0 \tag{10}$$

in which "⟨ ⟩" refers to ensemble average. It is the second law of thermodynamics in the statistical view [18].

Here, we assume the four state points of the thermoelectric cycle are prescribed, which has been often adopted in both existing theoretical and experimental researches [13][25]. This assumption allows us to have a well-defined benchmark result in the infinite-time operating case (i.e., the reversible one in Sec. II) and facilitate the formulation derivation. Thus, for the isothermal process $\mathrm{A} \to \mathrm{B}$, the entropy balance equation should hold,

$$S_{\mathrm{H}} - S_{\mathrm{L}} = \Delta S = \Delta \tilde{S}_{\mathrm{re\_AB}} + \Delta \tilde{S}_{\mathrm{irr\_AB}} = \frac{\tilde{Q}_{\mathrm{AB}}}{T_{\mathrm{H}}} + \Delta \tilde{S}_{\mathrm{irr\_AB}} = \langle \frac{\tilde{Q}_{\mathrm{AB}}}{T_{\mathrm{H}}} \rangle + \langle \Delta \tilde{S}_{\mathrm{irr\_AB}} \rangle. \quad (11)$$

Combining Eqs. (9) and (11) yields,

$$\langle e^{\left(\frac{\tilde{Q}_{\mathrm{AB}}}{k_B T_{\mathrm{H}}}\right)} \rangle = e^{\left(\frac{\Delta S}{k_B}\right)}. \quad (12)$$

Following the same derivation, we have the equation of identical form as Eq. (12) for the isothermal process $\mathrm{C} \to \mathrm{D}$,

$$\langle e^{\left(\frac{\tilde{Q}_{\mathrm{CD}}}{k_B T_{\mathrm{L}}}\right)} \rangle = e^{\left(-\frac{\Delta S}{k_B}\right)}. \quad (13)$$

Then, combination of Eqs. (12) and (13) leads to

$$\langle e^{\left(\frac{\tilde{Q}_{\mathrm{AB}}}{k_B T_{\mathrm{H}}}\right)} \rangle \langle e^{\left(\frac{\tilde{Q}_{\mathrm{CD}}}{k_B T_{\mathrm{L}}}\right)} \rangle = 1. \quad (14)$$

We can define the deviation of heat flow with respect to its ensemble average as,

$$\begin{aligned} \delta \tilde{Q}_{\mathrm{AB}} &= \tilde{Q}_{\mathrm{AB}} - \langle \tilde{Q}_{\mathrm{AB}} \rangle, \\ \delta \tilde{Q}_{\mathrm{CD}} &= \tilde{Q}_{\mathrm{CD}} - \langle \tilde{Q}_{\mathrm{CD}} \rangle. \end{aligned} \quad (15)$$

Thus, Eq. (14) can be transformed to,

$$e^{\left(\frac{\langle \tilde{Q}_{\mathrm{AB}} \rangle}{k_B T_{\mathrm{H}}} + \frac{\langle \tilde{Q}_{\mathrm{CD}} \rangle}{k_B T_{\mathrm{L}}}\right)} \langle e^{\left(\frac{\delta \tilde{Q}_{\mathrm{AB}}}{k_B T_{\mathrm{H}}}\right)} \rangle \langle e^{\left(\frac{\delta \tilde{Q}_{\mathrm{CD}}}{k_B T_{\mathrm{L}}}\right)} \rangle = 1. \quad (16)$$

According to the energy conservation law for the cycle, we have

$$\langle \widetilde{W} \rangle = \langle \tilde{Q}_{\mathrm{AB}} \rangle + \langle \tilde{Q}_{\mathrm{CD}} \rangle, \tag{17}$$

in which $\langle \widetilde{W} \rangle$ is the ensemble-average work. Substituting Eq. (17) into Eq. (16), we have,

$$\langle \widetilde{W} \rangle = \eta_{\mathrm{CA}} \langle \tilde{Q}_{\mathrm{AB}} \rangle - k_B T_{\mathrm{L}} \ln \left\{ \langle e^{\left(\frac{\delta \tilde{Q}_{\mathrm{AB}}}{k_B T_{\mathrm{H}}}\right)} \rangle \langle e^{\left(\frac{\delta \tilde{Q}_{\mathrm{CD}}}{k_B T_{\mathrm{L}}}\right)} \rangle \right\}. \tag{18}$$

Using the entropy balance equations,

$$\begin{aligned} \Delta S &= \langle \frac{\tilde{Q}_{\mathrm{AB}}}{T_{\mathrm{H}}} \rangle + \langle \Delta \tilde{S}_{\mathrm{irr\_AB}} \rangle, \\ -\Delta S &= \langle \frac{\tilde{Q}_{\mathrm{CD}}}{T_{\mathrm{L}}} \rangle + \langle \Delta \tilde{S}_{\mathrm{irr\_CD}} \rangle, \end{aligned} \tag{19}$$

we have,

$$\langle e^{\left(\frac{\delta \tilde{Q}_{\mathrm{AB}}}{k_B T_{\mathrm{H}}}\right)} \rangle = e^{\left(\frac{\langle \Delta \tilde{S}_{\mathrm{irr\_AB}} \rangle}{k_B}\right)}, \tag{20}$$

$$\langle e^{\left(\frac{\delta \tilde{Q}_{\mathrm{CD}}}{k_B T_{\mathrm{L}}}\right)} \rangle = e^{\left(\frac{\langle \Delta \tilde{S}_{\mathrm{irr\_CD}} \rangle}{k_B}\right)}. \tag{21}$$

Substituting Eqs. (20) & (21) into Eq. (18), we reach the formulation involving the irreversible work for our thermoelectric cycle,

$$\langle \widetilde{W} \rangle = \eta_{\mathrm{CA}} \langle \tilde{Q}_{\mathrm{AB}} \rangle - T_{\mathrm{L}} \{ \langle \Delta \tilde{S}_{\mathrm{irr\_AB}} \rangle + \langle \Delta \tilde{S}_{\mathrm{irr\_CD}} \rangle \}, \tag{22}$$

which holds the identical form to that of the widely-adopted one, except for the ensemble average. In this way, the conditions for guaranteeing the validity of Eq. (22), which employs entropy production to analyze the finite-time thermoelectric cycle, can be clarified on the basis of FTs, and they should be consistent with those for Eq. (8).

In order to discuss the power of such thermoelectric cycle, we need to specify how the entropy production of isothermal processes varying with the operating time interval $\tau$. According to Ref. [26], the entropy production rate during a process should

be equal to the product of driven force and flow rate, in spite of nonlinear or linear. Therefore, for the isothermal process devised in Fig. 2, the entropy production rate at the time $t$ could be expressed as,

$$\tilde{\sigma}(t) = \frac{\widetilde{\Delta\mu_{\Psi i}}}{T}\frac{\widetilde{\partial N}}{\partial t}, \tag{23}$$

in which $T$ is the temperature, and $\widetilde{\Delta\mu_{\Psi i}}$ is the electrochemical potential difference between the targeted system $\Psi$ and the $i$ th reservoir connecting with it at $t$. We could have the ensemble average of entropy production rate as,

$$\langle\tilde{\sigma}\rangle = \langle\frac{\widetilde{\Delta\mu_{\Psi\iota}}}{T}\frac{\widetilde{\partial N}}{\partial t}\rangle = \frac{\langle\widetilde{\Delta\mu_{\Psi\iota}}\rangle}{T}\langle\frac{\widetilde{\partial N}}{\partial t}\rangle + c_{\text{en\_cov}}(\frac{\widetilde{\Delta\mu_{\Psi\iota}}}{T}, \frac{\widetilde{\partial N}}{\partial t}), \tag{24}$$

with the ensemble-average covariance $c_{\text{en\_cov}}(\quad)$. It should be reasonable that the flow and its corresponding driven force is positively correlated, and thus we have

$$c_{\text{en\_cov}}\left(\frac{\widetilde{\Delta\mu_{\Psi\iota}}}{T}, \frac{\widetilde{\partial N}}{\partial t}\right) \geq 0 \rightarrow \langle\tilde{\sigma}\rangle = \langle\frac{\widetilde{\Delta\mu_{\Psi\iota}}}{T}\frac{\widetilde{\partial N}}{\partial t}\rangle \geq \frac{\langle\widetilde{\Delta\mu_{\Psi\iota}}\rangle}{T}\langle\frac{\widetilde{\partial N}}{\partial t}\rangle. \tag{25}$$

We could thus estimate a lower bound for the ensemble average of total entropy production for an isothermal process with the duration $\tau$,

$$\langle\Delta\tilde{S}_{\text{irr}}\rangle = \int_0^\tau \langle\tilde{\sigma}\rangle\, dt \geq \frac{1}{T}\int_0^\tau \langle\widetilde{\Delta\mu_{\Psi\iota}}\rangle\langle\frac{\widetilde{\partial N}}{\partial t}\rangle\, dt. \tag{26}$$

Taking the time average of total entropy production yields,

$$\left[\langle\Delta\tilde{S}_{\text{irr}}\rangle\right]_\tau = \frac{\langle\Delta\tilde{S}_{\text{irr}}\rangle}{\tau} \geq \frac{1}{T}\frac{1}{\tau}\int_0^\tau \langle\widetilde{\Delta\mu_{\Psi\iota}}\rangle\langle\frac{\widetilde{\partial N}}{\partial t}\rangle\, dt = \frac{1}{T}\left[\langle\widetilde{\Delta\mu_{\Psi\iota}}\rangle\langle\frac{\widetilde{\partial N}}{\partial t}\rangle\right]_\tau. \tag{27}$$

in which the symbol "$[\quad]_\tau$" refers to the time average. Similarly, we could have

$$\left[\langle\Delta\tilde{S}_{\text{irr}}\rangle\right]_\tau \geq \frac{1}{T}\left[\langle\widetilde{\Delta\mu_{\Psi i}}\rangle\langle\frac{\widetilde{\partial N}}{\partial t}\rangle\right]_\tau = \frac{1}{T}\left[\langle\widetilde{\Delta\mu_{\Psi i}}\rangle\right]_\tau\left[\langle\frac{\widetilde{\partial N}}{\partial t}\rangle\right]_\tau + \frac{1}{T}c_{\tau\_\text{cov}}\left(\langle\widetilde{\Delta\mu_{\Psi i}}\rangle, \langle\frac{\widetilde{\partial N}}{\partial t}\rangle\right), \tag{28}$$

where "$c_{\tau\_\text{cov}}(\quad)$" means the time average covariance. The ensemble averages of the

flow and its driven force are also supposed to be positively correlated during the evolution, which results in,

$$\left[\langle \Delta \tilde{S}_{\mathrm{irr}} \rangle\right]_{\tau} \geq \frac{1}{T}\left[\langle \widetilde{\Delta \mu_{\Psi_l}} \rangle \langle \frac{\widetilde{\partial N}}{\partial t} \rangle\right]_{\tau} \geq \frac{1}{T}\left[\langle \widetilde{\Delta \mu_{\Psi_l}} \rangle\right]_{\tau}\left[\langle \frac{\widetilde{\partial N}}{\partial t} \rangle\right]_{\tau}. \tag{29}$$

Herein, an average effective electrical resistance $R_{\mathrm{e}}$ is introduced to characterize the charge transport impedance between the targeted system and the reservoirs over the isothermal process,

$$R_{\mathrm{e}} = \frac{\left[\langle \widetilde{\Delta \mu_{\Psi_l}} \rangle\right]_{\tau}}{q_{\mathrm{e}}^2 \left[\langle \frac{\widetilde{\partial N}}{\partial t} \rangle\right]_{\tau}}, \tag{30}$$

in which $q_{\mathrm{e}}$ is the elementary charge. This average effective electrical resistance $R_{\mathrm{e}}$ is measurable and holds the comparable meaning with the conventional electrical resistance. Assume that in the view of time and ensemble average the charge transfer process is linear and thus $R_{\mathrm{e}}$ is independent on either $\left[\langle \widetilde{\Delta \mu_{\Psi_l}} \rangle\right]_{\tau}$ or $\left[\langle \frac{\widetilde{\partial N}}{\partial t} \rangle\right]_{\tau}$. Then, Eq. (29) becomes,

$$\left[\langle \Delta \tilde{S}_{\mathrm{irr}} \rangle\right]_{\tau} \geq \frac{q_{\mathrm{e}}^2}{T} R_{\mathrm{e}} \left[\langle \frac{\widetilde{\partial N}}{\partial t} \rangle\right]_{\tau}^{2}. \tag{31}$$

Since the four state points of the thermoelectric cycle are fixed, we could estimate the average charge flows for the processes $\mathrm{A} \rightarrow \mathrm{B}$ and $\mathrm{C} \rightarrow \mathrm{D}$ as,

$$\begin{aligned} \left[\langle \frac{\widetilde{\partial N}}{\partial t} \rangle\right]_{\tau_{\mathrm{AB}}} &\approx \frac{N_{\mathrm{B}} - N_{\mathrm{A}}}{\tau} = \frac{\Delta N_{\mathrm{AB}}}{\tau}, \\ \left[\langle \frac{\widetilde{\partial N}}{\partial t} \rangle\right]_{\tau\_\mathrm{AB}} &\approx \frac{N_{\mathrm{D}} - N_{\mathrm{C}}}{\tau} = \frac{\Delta N_{\mathrm{CD}}}{\tau}. \end{aligned} \tag{32}$$

In this way, we could reach a least estimation of the entropy production dependent on the duration $\tau$ for the two isothermal processes through combining Eqs. (31) & (32),

$$\langle \Delta \tilde{S}_{\mathrm{irr\_AB}} \rangle \geq \frac{1}{\tau} \frac{q_{\mathrm{e}}^2}{T_{\mathrm{H}}} R_{\mathrm{e\_AB}} \Delta N_{\mathrm{AB}}^2 \propto \tau^{-1},$$
$$\langle \Delta \tilde{S}_{\mathrm{irr\_CD}} \rangle \geq \frac{1}{\tau} \frac{q_{\mathrm{e}}^2}{T_{\mathrm{L}}} R_{\mathrm{e\_CD}} \Delta N_{\mathrm{CD}}^2 \propto \tau^{-1}, \tag{33}$$

which have the $\tau^{-1}$ scaling relation that has been extensively employed when analyzing the thermal engines of finite-time thermodynamics [12][13][15][27]. Thus, the work of the finite-time thermoelectric cycle could be estimated as,

$$\langle \widetilde{W} \rangle = \eta_{\mathrm{C}} \langle \tilde{Q}_{\mathrm{AB}} \rangle - T_{\mathrm{L}} q_{\mathrm{e}}^2 \left\{ \frac{R_{\mathrm{e\_AB}} \Delta N_{\mathrm{AB}}^2}{T_{\mathrm{H}}} + \frac{R_{\mathrm{e\_CD}} \Delta N_{\mathrm{CD}}^2}{T_{\mathrm{L}}} \right\} \tau^{-1}, \tag{34}$$

with the heat flow $\langle \tilde{Q}_{\mathrm{AB}} \rangle$ as,

$$\langle \tilde{Q}_{\mathrm{AB}} \rangle = T_{\mathrm{H}} \Delta S - T_{\mathrm{H}} \langle \Delta \tilde{S}_{\mathrm{irr\_AB}} \rangle = T_{\mathrm{H}} \Delta S - q_{\mathrm{e}}^2 R_{\mathrm{e\_AB}} \Delta N_{\mathrm{AB}}^2 \tau^{-1}. \tag{35}$$

The power can be calculated readily from Eq. (34) by dividing the cycle operation duration. With the assumption that the processes $\mathrm{B} \rightarrow \mathrm{C}$ and $\mathrm{D} \rightarrow \mathrm{A}$ are ideally adiabatic, we could neglect their duration $\tau_{\mathrm{adia}}$ for simplicity without altering the physical essence, and thus have,

$$\langle \tilde{P} \rangle = \frac{1}{2} \left\{ \eta_{\mathrm{C}} T_{\mathrm{H}} \Delta S \tau^{-1} - q_{\mathrm{e}}^2 \left\{ R_{\mathrm{e\_AB}} \Delta N_{\mathrm{AB}}^2 + R_{\mathrm{e\_CD}} \Delta N_{\mathrm{CD}}^2 \right\} \tau^{-2} \right\}. \tag{36}$$

Taking $\partial \langle \tilde{P} \rangle / \partial (\tau^{-1}) = 0$, we can determine the maximum power of the thermoelectric cycle, which reads,

$$\langle \tilde{P} \rangle_{\mathrm{Max}} = \frac{1}{8 R_{\mathrm{e\_AB}} q_{\mathrm{e}}^2 \Delta N_{\mathrm{AB}}^2} \frac{(\Delta S)^2}{1+\gamma} (T_{\mathrm{H}} - T_{\mathrm{L}})^2, \tag{37}$$

with

$$\tau_{\mathrm{MP}}^{-1} = \frac{1}{2 R_{\mathrm{e\_AB}} q_{\mathrm{e}}^2 \Delta N_{\mathrm{AB}}^2} \frac{\Delta S}{1+\gamma} (T_{\mathrm{H}} - T_{\mathrm{L}}). \tag{38}$$

The corresponding efficiency is given by,

$$\langle \eta \rangle_{\mathrm{MP}} = \frac{\eta_{\mathrm{C}}}{2 - \eta_{\mathrm{C}} / \{1+\gamma\}}, \tag{39}$$

with

$$\gamma = \frac{R_{\mathrm{e\_CD}}\Delta N_{\mathrm{CD}}^2}{R_{\mathrm{e\_AB}}\Delta N_{\mathrm{AB}}^2}. \tag{40}$$

When we define $\beta = 1 + \gamma$, Eq. (39) is well consistent with the efficiency formulation $\eta_{\mathrm{ST}}$ derived from Brownian motors as presented in Tab.1. This is reasonable due to the equivalence of varied types of heat engines. The corresponding maximum power of thermoelectricity holds the same explicit temperature dependence and the identical factor, i.e. 1/8, as that derived from stochastic thermodynamics.

For further clarifying the physical essence of the coefficient $\gamma$ for thermoelectricity, some transformations are introduced to make it more understandable and calculable for a specific TEG. Referring to Ref. [4], a Peltier coefficient can be defined in a reversible way for a thermoelectric system by constructing the isothermal process, which is given by,

$$\Pi = \frac{T\Delta S}{q_{\mathrm{e}}\Delta N}, \tag{41}$$

in which $\Delta S$ and $\Delta N$ are the entropy change and the charge number change of isothermal process at the temperature *T*. Using the Kelvin relation presented in the same paper [4], a Seebeck coefficient can be deduced as well,

$$\alpha_{\mathrm{S\_r}} = \frac{\Delta S}{q_{\mathrm{e}}\Delta N}. \tag{42}$$

Then, referring to Eq. (42), we could have,

$$\gamma = \frac{R_{\mathrm{e\_CD}}}{R_{\mathrm{e\_AB}}}\left(\frac{\Delta S/(q_{\mathrm{e}}\Delta N_{\mathrm{AB}})}{\Delta S/(q_{\mathrm{e}}\Delta N_{\mathrm{CD}})}\right)^2 = \frac{\alpha_{\mathrm{S\_r(AB)}}^2/R_{\mathrm{e\_AB}}}{\alpha_{\mathrm{S\_r(CD)}}^2/R_{\mathrm{e\_CD}}} = \frac{P_{\mathrm{F\_r(AB)}}}{P_{\mathrm{F\_r(CD)}}}, \tag{43}$$

where $P_{\mathrm{F\_r(AB)}} = \alpha_{\mathrm{S\_r(AB)}}^2/R_{\mathrm{e\_AB}}$ and $P_{\mathrm{F\_r(CD)}} = \alpha_{\mathrm{S\_r(CD)}}^2/R_{\mathrm{e\_CD}}$ should have the comparable physical contents to the thermoelectric power factor for the processes

$\mathrm{A} \to \mathrm{B}$ and $\mathrm{C} \to \mathrm{D}$, respectively. Therefore, we could say the coefficient $\gamma$ is the ratio of such thermoelectric power factors at the high and low temperatures. Moreover, the maximum power of the thermoelectric cycle can be rewritten to a compact expression,

$$\langle \tilde{P} \rangle_{\mathrm{Max}} = \frac{1}{8(1+\gamma)} P_{\mathrm{F\_r(AB)}} (T_{\mathrm{H}} - T_{\mathrm{L}})^2. \tag{44}$$

In practice, the difference of $P_{\mathrm{F\_r}}$ at the high and low temperature is frequently assumed to be non-significant, resulting in the nearly symmetric dispassion condition ($\gamma \approx 1$), and thus we have,

$$\langle \eta \rangle_{\mathrm{MP}} = \frac{\eta_{\mathrm{C}}}{2 - \eta_{\mathrm{C}}/2}, \tag{45}$$

$$\langle \tilde{P} \rangle_{\mathrm{Max}} = \frac{1}{16} P_{\mathrm{F\_r(AB)}} (T_{\mathrm{H}} - T_{\mathrm{L}})^2, \tag{46}$$

which are distinct compared to the formulations based the linear-irreversible and endoreversible thermodynamics at the identical condition.

## IV. Discussions

### *A. Comparison to the linear-irreversible-thermodynamics-based formulations*

The maximum power-efficiency pair of finite-time thermoelectric cycle can well agree with that derived from the stochastic thermodynamics, but poses the discrepancy with the linear-irreversible-thermodynamics-based formulations that have been widely adopted in the research of thermoelectricity [6]. Firstly, we should note that the steady-state TEG generally serves as the targeted system in the linear-irreversible-thermodynamic analysis, and its power output is continuous; by contrast, the power output pattern should be discontinuous for a thermodynamic cycle, as shown in Fig. 4 (a). In order to have continuous power output, we can combine the thermoelectric cycle with another cycle of phase lag, as given in Fig. 4

(b), and thus the power is doubled, while the efficiency remains unchanged:

$$\langle \tilde{P} \rangle_{\mathrm{Max}}^{(\mathrm{Cont})} = \frac{1}{4}\frac{1}{(1+\gamma)} P_{\mathrm{F\_r(AB)}} (T_{\mathrm{H}} - T_{\mathrm{L}})^2. \tag{47}$$

Table 2 demonstrates the expressions of the efficiency at max power and the continuous max power with the parameter $\gamma$ at the different limits: when the high-temperature-side dissipation dominates, i.e. $\gamma \to 0$, the continuous power of thermoelectric cycle has the same form as the linear-irreversible-thermodynamics case, but the corresponding efficiency is not $\eta_{\mathrm{C}}/2$; by contrast, when the low-temperature-side dissipation is dominant, i.e. $\gamma \to \infty$, the efficiency at max power given by the linear-irreversible thermodynamics can be recovered (that is, $\eta_{\mathrm{C}}/2$), while the power becomes 0. Note that these limiting values of $\gamma$ could be hard to be realistic for the practical TEGs, and thus such discussion makes sense majorly in the view of mathematics. Actually, the derivation in the linear-irreversible thermodynamics generally assumes the condition of symmetric dispassion ($\gamma = 1$), where the thermoelectric cycle holds the different continuous max power and efficiency compared to the linear-irreversible-thermodynamics formulations.

TABLE 2 Efficiency at max power and continuous max power with the parameter γ at the different limits.

| | **Description** | **Continuous max power** | **Efficiency at max power** |
|---|---|---|---|
| $\gamma \to 0$ | High-temperature-side dissipation dominates | $\frac{P_{\mathrm{F\_r(AB)}}}{4}(T_{\mathrm{H}} - T_{\mathrm{L}})^2$ | $\frac{\eta_{\mathrm{C}}}{2 - \eta_{\mathrm{C}}}$ |
| $\gamma \to \infty$ | Low-temperature-side dissipation dominates | 0 | $\frac{\eta_{\mathrm{C}}}{2}$ |
| $\gamma = 1$ | Symmetric dispassion | $\frac{P_{\mathrm{F\_r(AB)}}}{8}(T_{\mathrm{H}} - T_{\mathrm{L}})^2$ | $\frac{\eta_{\mathrm{C}}}{2 - \eta_{\mathrm{C}}/2}$ |

In order to explain such incompatibility, we notice the discrepancy of thermoelectric coefficients (i.e., Peltier and Seebeck) in the thermoelectric cycle, compared to the linear-irreversible thermodynamics analysis. Referring to Eq. (41), the Peltier coefficient (Π) here is derived from the reversible heat flow, corresponding to the Seebeck coefficient ($\alpha_{\mathrm{S\_r}}$) defined with respective to the entropy change $\Delta S$ that is the difference of the state variable, entropy *S*, as given in Eq. (42); by contrast, the Peltier coefficient (denoted by $\Pi_{\mathrm{irr}}$) used in the linear irreversible thermodynamics relates the heat flow $\langle \tilde{Q} \rangle$ to the accumulated current [6],

$$\Pi_{\mathrm{irr}} = \frac{\langle \tilde{Q} \rangle}{q_{\mathrm{e}} \Delta N}. \tag{48}$$

Accordingly, in terms of the ORR, the Seebeck coefficient (denoted by $\alpha_{\mathrm{S\_irr}}$) in the linear irreversible thermodynamics is dependent on the entropy flow, $\langle \tilde{Q}/T \rangle$ [6], which excludes the entropy production in the entropy change $\Delta S$,

$$\alpha_{\mathrm{S\_irr}} = \frac{\langle \tilde{Q}/T \rangle}{q_{\mathrm{e}} \Delta N}. \tag{49}$$

If we substitute the Peltier coefficient, $\Pi_{\mathrm{irr}}$, into the work expression of the finite-time thermoelectric cycle, Eq. (34), we have,

$$\langle \tilde{W} \rangle = \eta_{\mathrm{C}} \Pi_{\mathrm{irr}} q_{\mathrm{e}} \Delta N_{\mathrm{AB}} - q_{\mathrm{e}}^2 R_{\mathrm{e\_AB}} \Delta N_{\mathrm{AB}}^2 \{1 - \eta_{\mathrm{C}} + \gamma\} \tau^{-1}. \tag{50}$$

Following the widely-employed assumption in the linear-irreversible thermodynamics that the thermoelectric coefficients are constant, we can derive the maximum power-efficiency pair accordingly,

$$\langle \tilde{P} \rangle_{\mathrm{Max\_irr}}^{(\mathrm{Cont})} = \frac{1}{4} \frac{1}{1 - \eta_{\mathrm{C}} + \gamma} P_{\mathrm{F\_irr(AB)}} (T_{\mathrm{H}} - T_{\mathrm{L}})^2, \tag{51}$$

$$\langle \eta \rangle_{\mathrm{MP\_irr}} = \frac{\eta_{\mathrm{C}}}{2}. \tag{52}$$

Then, at the symmetric dispassion condition, $\gamma = 1$, the maximum power-efficiency pair of the thermoelectric cycle with $\Pi_{\rm irr}$ and $\alpha_{\rm S\_irr}$ reaches,

$$\langle \tilde{P} \rangle_{\rm Max\_irr}^{\rm (Cont)} = \frac{1}{4}\frac{1}{2-\eta_{\rm C}} P_{\rm F\_irr(AB)} (T_{\rm H} - T_{\rm L})^2 \leq \frac{1}{4} P_{\rm F\_irr(AB)} (T_{\rm H} - T_{\rm L})^2,$$
$$\langle \eta \rangle_{\rm MP\_irr} = \frac{\eta_{\rm C}}{2}, \tag{53}$$

which is in the identical form of the linear-irreversible-thermodynamics formulations given in Tab.1. Actually, it requires further clarification on which definition of thermoelectric coefficients is more proper for accessing the efficiency of TEGs.

### *B. Comparison to the endoreversible-thermodynamics-based formulations*

Here, we argue the applicability using the endoreversible thermodynamics to analyze the Carnot-like thermoelectric cycle. The hypothesis of endoreversibility, which merely considers the irreversibility emerging due to the finite heat exchange with heat reservoirs [8], is fundamentally distinct with the thermoelectric cycle here where the irreversibility arises from the internal processes [5]. Moreover, the heat input and output in the thermoelectric cycle here are achieved through the Peltier effect rather than to the finite heat exchange, which does not give a place for using the endoreversible assumption.

In fact, if only considering the mathematical expressions, the difference of the maximum power-efficiency pair between the thermoelectric cycle and the endoreversible thermodynamics could be eliminated with assuming,

$$\gamma = \sqrt{T_{\rm L}/T_{\rm H}} = \frac{P_{\rm F\_r(AB)}}{P_{\rm F\_r(CD)}}, \tag{54}$$

which leads to,

$$\langle \tilde{P} \rangle_{\mathrm{Max}} = \frac{1}{8} P_{\mathrm{F\_r(AB)}} T_{\mathrm{H}} \eta_{\mathrm{CA}} \left( \sqrt{T_{\mathrm{H}}} - \sqrt{T_{\mathrm{L}}} \right)^2, \tag{55}$$

$$\langle \eta \rangle_{\mathrm{MP}} = \frac{\eta_{\mathrm{C}}}{2 - \eta_{\mathrm{C}} / \{1 + \gamma\}} = \frac{\eta_{\mathrm{C}}}{1 + \sqrt{T_{\mathrm{L}} / T_{\mathrm{H}}}} = 1 - \sqrt{T_{\mathrm{L}} / T_{\mathrm{H}}}\,. \tag{56}$$

Nevertheless, such coincidence might not be that physically rational. In addition of the argument above, the ratio of thermoelectric power factors at the high and low temperatures generally approximates 1.0, $\gamma \approx 1$, in practice, which makes it kind of hard to give a solid explanation about the physical or practical essence of $\gamma = \sqrt{T_{\mathrm{L}} / T_{\mathrm{H}}}$.

### *C. Implementation of the present formulations for realistic thermoelectric material*

Our discussions above are conducted in a rather theoretic view of thermodynamics, while this section presents how to effectively implement our models, i.e. Eqs. (39) & (47), to estimate the maximum power-efficiency pairs of realistic thermoelectric materials based on the finite-time Carnot-like thermoelectric cycle.

To do so, we need to firstly identify those two parameters (the power factor $P_{\mathrm{F\_r}}$ and the coefficient $\gamma$) embedded in Eqs. (39) & (47) for a specific material. As clarified above, the Seebeck coefficient in the present formulations holds the different physical essences compared with conventionally-used one. In terms of our previous work [4] that built the reversible quasi-static process for Seebeck phenomenon, this reversible Seebeck coefficient can be expressed as,

$$\alpha_{\mathrm{S\_r}} = \frac{1}{q_{\mathrm{e}}} \left( \left. \frac{dN}{dT} \right|_{\mu} \right) \Big/ \left( \left. \frac{dN}{d\mu} \right|_{T} \right), \tag{57}$$

with

$$N = \int f_{\mathrm{FD}} D(\varepsilon_{\mathbf{k}}) d\varepsilon_{\mathbf{k}} = \int \frac{2}{e^{\left(\frac{\varepsilon_{\mathbf{k}}-\mu}{k_{\mathrm{B}}T}\right)}+1} D(\varepsilon_{\mathbf{k}}) d\varepsilon_{\mathbf{k}}, \tag{58}$$

and the Fermi-Dirac distribution,

$$f_{\mathrm{FD}} = \frac{1}{e^{\left(\frac{\varepsilon_{\mathbf{k}}-\mu}{k_{\mathrm{B}}T}\right)}+1}, \tag{59}$$

in which $\varepsilon_{\mathbf{k}}$ is the carrier energy and $D(\varepsilon_{\mathbf{k}})$ is the density of states (DOS). Thus, we have

$$\alpha_{\mathrm{S\_r}} = \frac{1}{q_{\mathrm{e}}T} \frac{\int f_{\mathrm{FD}}[1-f_{\mathrm{FD}}][\varepsilon_{\mathbf{k}}-\mu] D(\varepsilon_{\mathbf{k}}) d\varepsilon_{\mathbf{k}}}{\int f_{\mathrm{FD}}[1-f_{\mathrm{FD}}] D(\varepsilon_{\mathbf{k}}) d\varepsilon_{\mathbf{k}}}. \tag{60}$$

Compared to the generally-used Seebeck coefficient model that is derived from the Boltzmann transport equation [28], the terms of group velocity and relaxation time, which closely relates to the irreversible transport mechanisms, are dropped in this reversible formula, Eq. (60). This is reasonable, since the reversible Seebeck coefficient is defined based on the quasi-static process [4] that eliminates the irreversibility. Actually, Peterson and Shastry [29] proposed the similar expression to Eq. (60) through the slow-limit simplification of the Kubo formula, and the authors named it Kelvin formula and regarded it as an approximate expression for the exact Seebeck coefficient, which means it might loss some accuracy. Nevertheless, based on our analysis, this reversible Seebeck coefficient, which is very concise, holds own physical content and can be utilized to estimate the maximum power-efficiency based on the finite-time thermodynamic cycle. As for the electrical resistivity term in the PF expression, the conventional resistivity could be adopted to characterize the irreversibility during the charge transport processes. Naturally, when such reversible thermoelectric power factor ($P_{\mathrm{F\_r}}$) is determined, the coefficient $\gamma$, i.e. the ratio of

thermoelectric power factors at the high and low temperatures, could be readily calculated.

As a case study, our models are applied to the n-type Silicon [28][30][31]. The energy band of Si is characterized by the parabolic model with the effective mass [32],

$$\varepsilon_{\mathbf{k}} = \frac{\hbar^2 \mathbf{k}^2}{2m_{\mathrm{e\_DOS}}} + E_{\mathrm{C}}. \tag{61}$$

Setting the minimum energy in the conduction band $E_{\mathrm{C}} = 0$, the DOS is given by

$$D(\varepsilon_{\mathbf{k}}) = \frac{1}{2\pi^2}\left(\frac{2m_{\mathrm{e\_DOS}}}{\hbar^2}\right)^{3/2}\sqrt{\varepsilon_{\mathbf{k}}}. \tag{62}$$

The Fermi level is calculated following Ref. [33], which is dependent on both the temperature and the doping concentration.

Figure 5 (a) compares the Seebeck coefficient values for the n-doped Silicon calculated by the reversible formulation, Eq. (60), and measured by the experiments [28][30], respectively. It is found that the reversible Seebeck coefficients are very close to the experimental ones for the highly-doped case (the doping concentration $n_{\mathrm{d}}$ = 6.0e19 cm$^{-3}$), where the diffusion component dominates [28]. By contrast, the reversible Seebeck coefficient values of the lightly-doped sample the doping concentration $n_{\mathrm{d}}$ = 2.6e15 cm$^{-3}$) can significantly deviate the experimental data. This is because the measured Seebeck coefficients of the lightly-doped Silicon generally involves a big portion of phonon-drag term [30] which is attributed to the momentum exchange between the carriers and the non-equilibrium phonon system. This irreversible factor is not included in the present model. In fact, such limit could not significantly affect the utilization of our model in practice, which can serve as an

effective and concise alternative for performance evaluation, since the thermoelectric materials for the practical applications are frequently medium- or highly-doped [34].

Therefore, here we focus on the highly-doped Silicon ($n_{\mathrm{d}} \geq$ 1.0e19 cm$^{-3}$), of which resistivity could be estimated using the mobility [31],

$$\rho_{\mathrm{e}} = \frac{1}{q_{\mathrm{e}} n_{\mathrm{e}} k_1} T^{3/2} \tag{63}$$

where $n_{\mathrm{e}}$ is the free-electron density (derived along with the Fermi level calculation) and $k_1 = 15\mathrm{e}5\ \ \mathrm{K}^{3/2}\mathrm{cm}^2/\mathrm{V/s}$ [31]. Then, the reversible power factors ($P_{\mathrm{F\_r}}$) can be calculated, and Fig. 5(b) shows $P_{\mathrm{F\_r}}$ decreases with the increasing temperature and the decreasing doping level.

Furthermore, we calculated the continuous maximum power-efficiency pair and the relevant parameters via the present model using the reversible Seebeck coefficient, with the cold source temperature fixed at 300 K. In Fig. 6(a), the coefficient $\gamma$ decreases with the increasing temperature and the decreasing doping concentration. The efficiency at maximum power increases with the heat source temperature and keeps under the Carnot efficiency curve, while the efficiency variation due to the doping concentration is minor. Figure 6(b) gives the continuous maximum power per leg length, and it can be enhanced with both the increasing heat source temperature and doping level.

## V. Conclusions

The present work constructs the Carnot-like thermoelectric cycle by designing a set of protocols for the isothermal and adiabatic processes of thermoelectricity, which has the Carnot efficiency and zero power in quasi-static case. The maximum

power-efficiency pair of finite-time thermoelectric cycle is derived on the basis of FT, which is identical to that obtained from the stochastic thermodynamics, but poses the discrepancy with the linear-irreversible-thermodynamics and the endoreversible-thermodynamics -based ones.

As comparing to the linear-irreversible-thermodynamics case, their incompatibility should be attributed to the difference in the definitions of Peltier and Seebeck coefficients: the thermoelectric coefficients in the thermoelectric cycle are derived based on the reversible heat flow, while those in the linear irreversible thermodynamics are relevant to the heat flow. Moreover, as for the endoreversible thermodynamics, the applicability of endoreversibility could be questionable for analyzing the thermoelectric cycle here, due to the incompatibility of endoreversible hypothesis that merely considers the irreversibility from the finite heat transfer between the thermal reservoirs, though the distinction of the mathematical expressions can vanish with assuming $\gamma = \sqrt{T_{\mathrm{L}}/T_{\mathrm{H}}}$ that could not be applicable for a practical TEG.

Lastly, we present how to utilize our models, Eqs. (39) & (47), as an effective and concise tool to estimate the maximum power-efficiency pairs of realistic thermoelectric materials via taking the n-type Silicon as the case study.

## Acknowledgements

This work is financially supported by Région Pays de la Loire France within the NExT2Talents program TOP-OPTIM project (998UMR6607 EOTP NEXINTERTALENTHUA).

# References


[1] L. E. Bell, “Cooling, heating, generating power, and recovering waste heat with thermoelectric systems,” *Science (80-. ).*, vol. 321, no. 5895, pp. 1457–1461, 2008, doi: 10.1126/science.1158899.

[2] Z. Liu *et al.*, “Evolution of Thermoelectric Generators: From Application to Hybridization,” *Small*, 2023, doi: 10.1002/smll.202304599.

[3] B. David, J. Ramousse, and L. Luo, “Optimization of thermoelectric heat pumps by operating condition management and heat exchanger design,” *Energy Convers. Manag.*, vol. 60, pp. 125–133, 2012, doi: 10.1016/j.enconman.2012.02.007.

[4] Y. C. Hua, T. W. Xue, and Z. Y. Guo, “Reversible reciprocal relation of thermoelectricity,” *Phys. Rev. E*, vol. 103, no. 1, pp. 1–23, 2021, doi: 10.1103/PhysRevE.103.012107.

[5] Y. Apertet, H. Ouerdane, C. Goupil, and P. Lecoeur, “Irreversibilities and efficiency at maximum power of heat engines: The illustrative case of a thermoelectric generator,” *Phys. Rev. E - Stat. Nonlinear, Soft Matter Phys.*, vol. 85, no. 3, pp. 1–5, 2012, doi: 10.1103/PhysRevE.85.031116.

[6] C. Goupil, W. Seifert, K. Zabrocki, E. Müller, and G. J. Snyder, “Thermodynamics of thermoelectric phenomena and applications,” *Entropy*, vol. 13, no. 8, pp. 1481–1517, 2011, doi: 10.3390/e13081481.

[7] I. I. Novikov, “The efficiency of atomic power stations (a review),” *J. Nucl. Energy*, vol. 7, no. 1–2, pp. 125–128, 1958, doi: 10.1016/0891-3919(58)90244-4.

[8] K. H. Hoffmann, “An introduction to endoreversible thermodynamics,” *AAPP Atti della Accad. Peloritana dei Pericolanti, Cl. di Sci. Fis. Mat. e Nat.*, vol. 86, no. SUPPL.1, pp. 1–18, 2008, doi: 10.1478/C1S0801011.

[9] U. Seifert, “Stochastic thermodynamics, fluctuation theorems and molecular machines,” *Reports Prog. Phys.*, vol. 75, no. 12, 2012, doi: 10.1088/0034-4885/75/12/126001.

[10] M. Esposito, R. Kawai, K. Lindenberg, and C. Van Den Broeck, “Quantum-dot Carnot engine at maximum power,” *Phys. Rev. E - Stat. Nonlinear, Soft Matter Phys.*, vol. 81, no. 4, 2010, doi: 10.1103/PhysRevE.81.041106.

[11] C. Van Den Broeck, “Thermodynamic efficiency at maximum power,” *Phys. Rev. Lett.*, vol. 95, no. 19, pp. 2–4, 2005, doi: 10.1103/PhysRevLett.95.190602.

[12] J. Kaur, R. S. Johal, and M. Feidt, “Thermoelectric generator in endoreversible approximation: The effect of heat-transfer law under finite physical dimensions constraint,” *Phys. Rev. E*, vol. 105, no. 3, 2022, doi: 10.1103/PhysRevE.105.034122.

[13] T. Schmiedl and U. Seifert, “Efficiency at maximum power: An analytically solvable model for stochastic heat engines,” *Epl*, vol. 81, no. 2, 2008, doi: 10.1209/0295-5075/81/20003.

[14] R. Fu and Q. Wang, “Stochastic control of thermodynamic heat engines,” *Annu. Rev. Control*, no. February, p. 100894, 2023, doi: 10.1016/j.arcontrol.2023.04.005.

[15] M. Esposito, R. Kawai, K. Lindenberg, and C. Van Den Broeck, “Efficiency at maximum power of low-Dissipation carnot engines,” *Phys. Rev. Lett.*, vol. 105, no. 15, pp. 1–4, 2010, doi: 10.1103/PhysRevLett.105.150603.

[16] G. E. Crooks, “Entropy production fluctuation theorem and the nonequilibrium work relation,” *Phys. Rev. E*, vol. 60, no. 3, pp. 2721–2726, 1999.

[17] C. Jarzynski, “Hamiltonian derivation of a detailed fluctuation theorem,” *J. Stat. Phys.*, vol. 98,

no. 1–2, pp. 77–102, 2000, doi: 10.1023/a:1018670721277.

[18] B. Palmieri and D. Ronis, “Jarzynski equality: Connections to thermodynamics and the second law,” *Phys. Rev. E - Stat. Nonlinear, Soft Matter Phys.*, vol. 75, no. 1, 2007, doi: 10.1103/PhysRevE.75.011133.

[19] C. Jarzynski, “Nonequilibrium equality for free energy differences,” *Phys. Rev. Lett.*, vol. 78, no. 14, pp. 2690–2693, 1997, doi: 10.1103/PhysRevLett.78.2690.

[20] G. Benenti, G. Casati, K. Saito, and R. S. Whitney, “Fundamental aspects of steady-state conversion of heat to work at the nanoscale,” *Phys. Rep.*, vol. 694, pp. 1–124, 2017, doi: 10.1016/j.physrep.2017.05.008.

[21] N. Merhav and Y. Kafri, “Statistical properties of entropy production derived from fluctuation theorems,” *J. Stat. Mech. Theory Exp.*, vol. 2010, no. 12, 2010, doi: 10.1088/1742-5468/2010/12/P12022.

[22] T. W. Xue and Z. Y. Guo, “Thermoelectric Cycle and the Second Law of Thermodynamics,” *Entropy*, vol. 25, no. 1, 2023, doi: 10.3390/e25010155.

[23] M. Campisi, P. Talkner, and P. Hänggi, “Fluctuation theorem for arbitrary open quantum systems,” *Phys. Rev. Lett.*, vol. 102, no. 21, pp. 1–4, 2009, doi: 10.1103/PhysRevLett.102.210401.

[24] D. Andrieux, P. Gaspard, T. Monnai, and S. Tasaki, “The fluctuation theorem for currents in open quantum systems,” *New J. Phys.*, vol. 11, 2009, doi: 10.1088/1367-2630/11/4/043014.

[25] V. Blickle and C. Bechinger, “Realization of a micrometre-sized stochastic heat engine,” *Nat. Phys.*, vol. 8, no. 2, pp. 143–146, 2012, doi: 10.1038/nphys2163.

[26] E. Solano-Carrillo and A. J. Millis, “Theory of entropy production in quantum many-body systems,” *Phys. Rev. B*, vol. 93, no. 22, 2016, doi: 10.1103/PhysRevB.93.224305.

[27] Y. H. Ma, R. X. Zhai, J. Chen, C. P. Sun, and H. Dong, “Experimental Test of the $1/\tau$ -Scaling Entropy Generation in Finite-Time Thermodynamics,” *Phys. Rev. Lett.*, vol. 125, no. 21, 2020, doi: 10.1103/PhysRevLett.125.210601.

[28] J. Sadhu *et al.*, “Quenched phonon drag in silicon nanowires reveals significant effect in the bulk at room temperature,” *Nano Lett.*, vol. 15, no. 5, pp. 3159–3165, 2015, doi: 10.1021/acs.nanolett.5b00267.

[29] M. R. Peterson and B. S. Shastry, “Kelvin formula for thermopower,” *Phys. Rev. B - Condens. Matter Mater. Phys.*, vol. 82, no. 19, 2010, doi: 10.1103/PhysRevB.82.195105.

[30] T. H. Geballe and G. W. Hull, “Seebeck effect in silicon,” *Phys. Rev.*, vol. 98, no. 4, pp. 940–947, 1955, doi: 10.1103/PhysRev.98.940.

[31] A. Stranz, J. Kähler, A. Waag, and E. Peiner, “Thermoelectric properties of high-doped silicon from room temperature to 900 K,” *J. Electron. Mater.*, vol. 42, no. 7, pp. 2381–2387, 2013, doi: 10.1007/s11664-013-2508-0.

[32] G. D. Mahan, L. Lindsay, and D. A. Broido, “The Seebeck coefficient and phonon drag in silicon,” *J. Appl. Phys.*, vol. 116, no. 24, 2014, doi: 10.1063/1.4904925.

[33] B. V. Zegbroeck, *Principles of Semiconductor Devices*. Online book, 2011.

[34] D. Narducci and F. Giulio, “Recent Advances on Thermoelectric Silicon for Low-Temperature Applications,” *Materials (Basel).*, vol. 15, no. 3, pp. 1–13, 2022, doi: 10.3390/ma15031214.

## Figure captions

Figure 1 Temperature (T) – Entropy (S) diagram of the Carnot cycle: $T_H$ the high temperature, $T_L$ the low temperature.

Figure 2 Isothermal process realization of a thermoelectric system within a time interval $\tau$: $T$ is temperature.

Figure 3 Adiabatic process realization of a thermoelectric system within a time interval $\tau_{adia}$.

Figure 4 (a) Schematic of the work evolution within single thermoelectric cycle, which corresponds to discontinuous power output; (b) Schematic of the work evolution when combining two cycles, which can have a continuous power output.

Figure 5 (a) Seebeck coefficients of n-doped Silicon at the varied doping concentrations ($n_d$) calculated by the reversible formulation, with comparison to the experimental data [28][30]; (b) Reversible power factor ($P_{F\_r}$) of highly-doped Silicon vs. temperature

Figure 6 Continuous maximum power and corresponding efficiency estimated by the present model using the revisable power factor for n-doped Silicon samples, with the cold source temperature equal to 300 K and the varied doping concentrations: (a) the coefficient $\gamma$ and the efficiencies at maximum power vs. heat source temperature; (b) Continuous maximum power per leg length vs. heat source temperature.

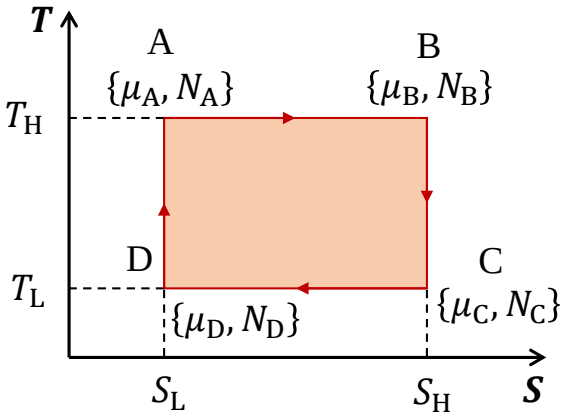


Figure 1 Temperature (T) – Entropy (S) diagram of the Carnot cycle: $T_H$ the high temperature, $T_L$ the low temperature.

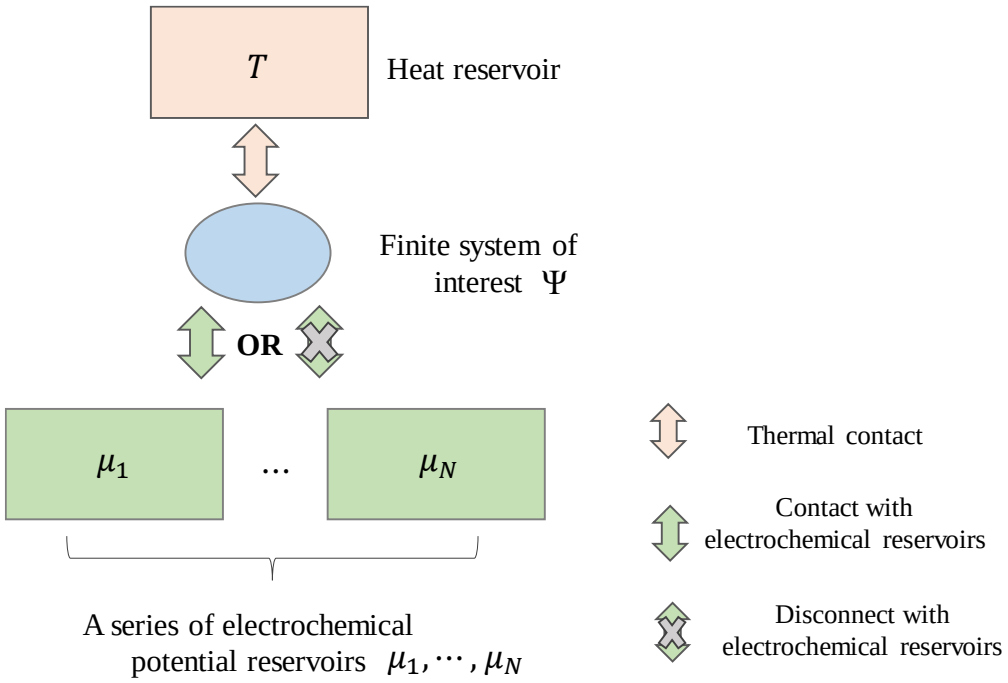


Figure 2 Isothermal process realization of a thermoelectric system within a time interval $\tau$: $T$ is temperature.

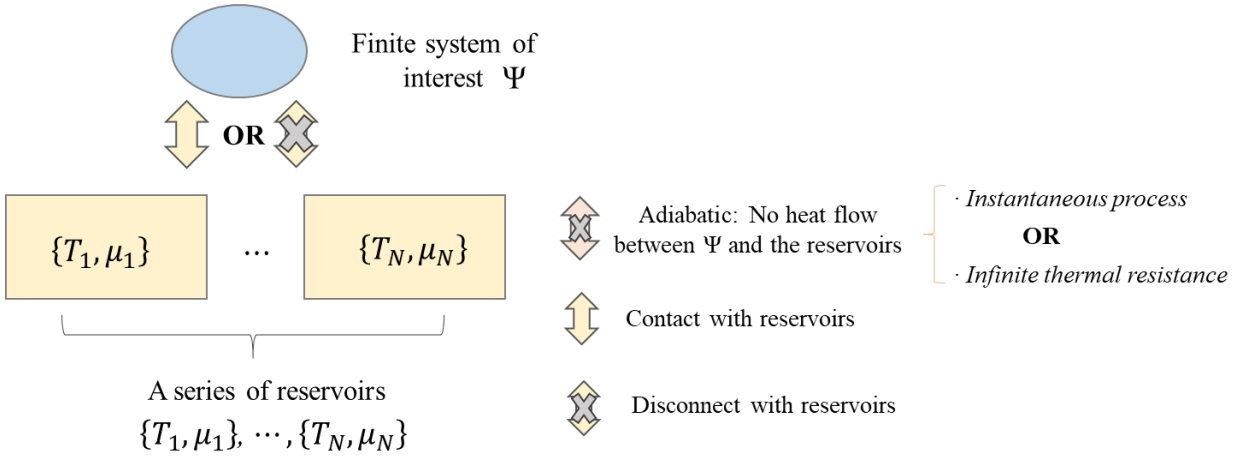


Figure 3 Adiabatic process realization of a thermoelectric system within a time interval $\tau_{\text{adia}}$.

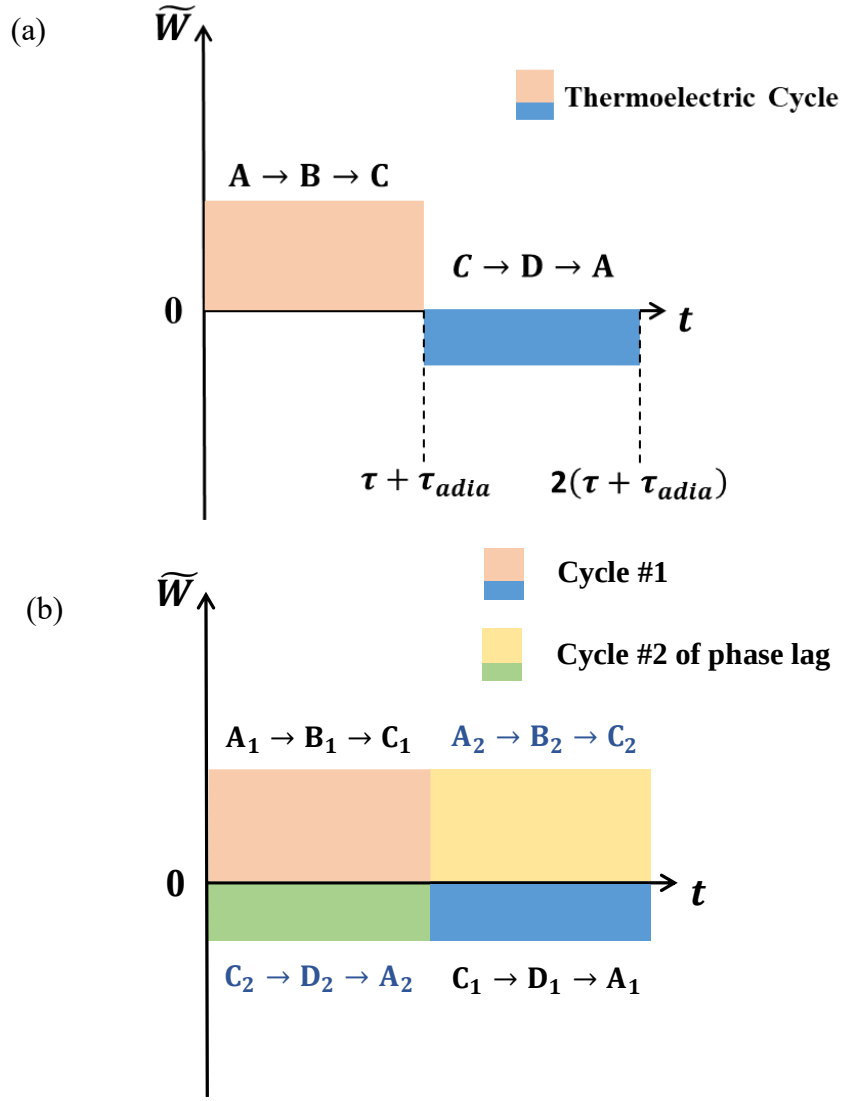


Figure 4 (a) Schematic of the work evolution within single thermoelectric cycle, which corresponds to discontinuous power output; (b) Schematic of the work evolution when combining two cycles, which can have a continuous power output.

(a)

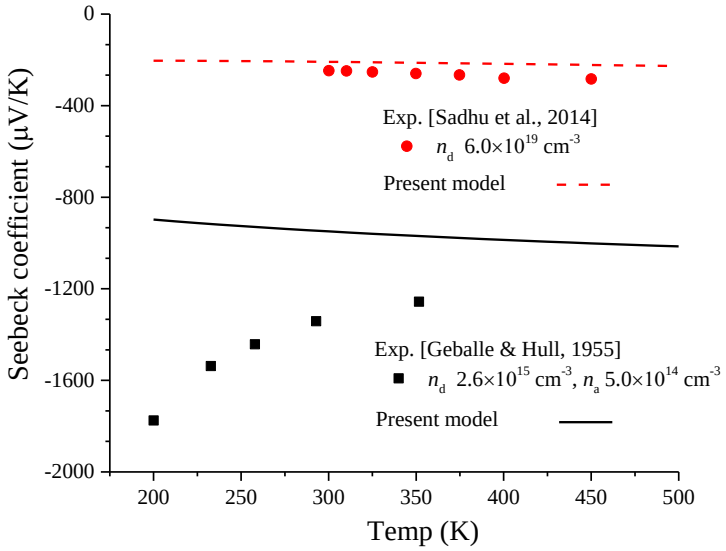


(b)

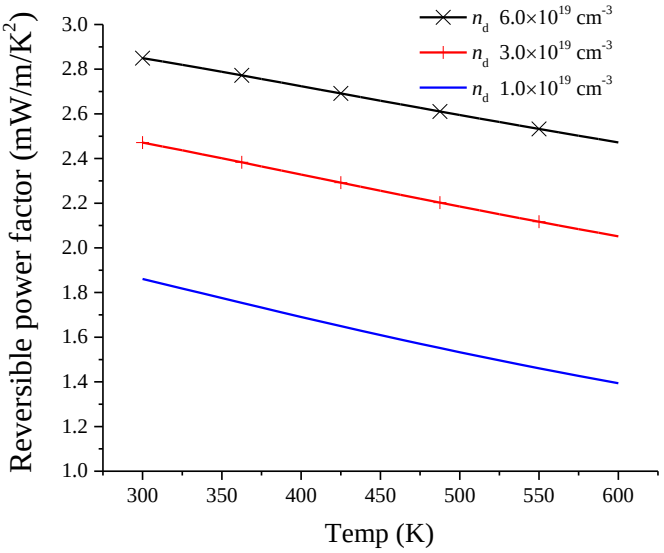


Figure 5 (a) Seebeck coefficients of n-doped Silicon at the varied doping concentrations ($n_d$) calculated by the reversible formulation, with comparison to the experimental data [28][30]; (b) Reversible power factor ($P_{F\_r}$) of highly-doped Silicon vs. temperature

(a)

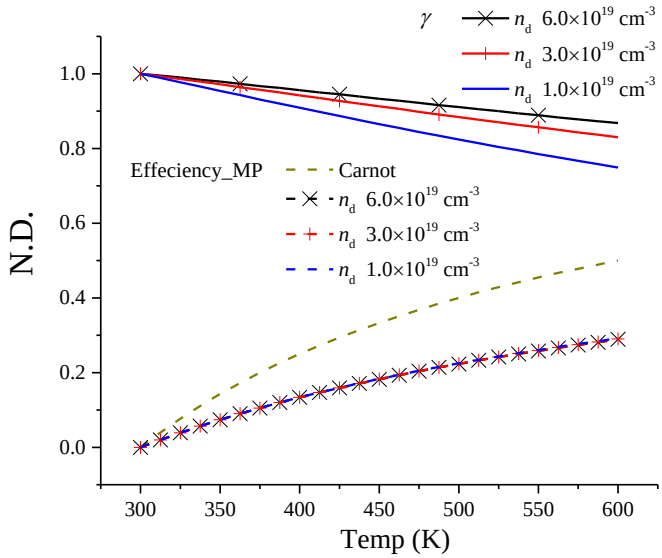


(b)

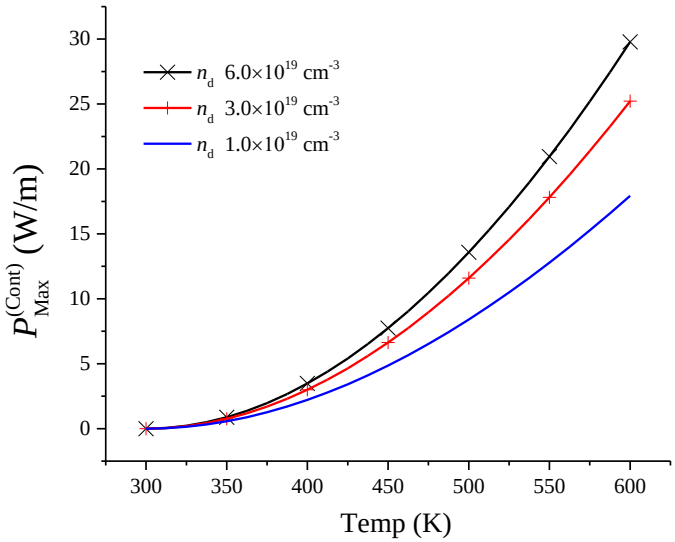


Figure 6 Continuous maximum power and corresponding efficiency estimated by the present model using the revisable power factor for n-doped Silicon samples, with the cold source temperature equal to 300 K and the varied doping concentrations: (a) the coefficient $\gamma$ and the efficiencies at maximum power vs. heat source temperature; (b) Continuous maximum power per leg length vs. heat source temperature.